



Isotopic composition of daily precipitation along the southern foothills of the Himalayas: impact of marine and continental sources of atmospheric moisture

Ghulam Jeelani¹, Rajendrakumar D. Deshpande², Michal Galkowski³, and Kazimierz Rozanski³

¹Department of Earth Sciences, University of Kashmir, Srinagar 190006, India

²Geosciences Division, Physical Research Laboratory (PRL), Navrangpura, Ahmedabad 380009, India

³Faculty of Physics and Applied Computer Science, AGH University of Science and Technology, Krakow 30-059, Poland

Correspondence: Ghulam Jeelani (geojeelani@gmail.com)

Received: 19 August 2017 – Discussion started: 21 September 2017

Revised: 9 April 2018 – Accepted: 6 June 2018 – Published: 22 June 2018

Abstract. The flow of the Himalayan rivers, a key source of fresh water for more than a billion people primarily depends upon the strength, behaviour and duration of the Indian summer monsoon (ISM) and the western disturbances (WD), two contrasting circulation regimes of the regional atmosphere. An analysis of the ²H and ¹⁸O isotope composition of daily precipitation collected along the southern foothills of the Himalayas, combined with extensive backward trajectory modelling, was used to gain deeper insight into the mechanisms controlling the isotopic composition of precipitation and the origin of atmospheric moisture and precipitation during ISM and WD periods. Daily precipitation samples were collected during the period from September 2008 to December 2011 at six stations, extending from Srinagar in the west (Kashmir state) to Dibrugarh in the east (Assam state). In total, 548 daily precipitation samples were collected and analysed for their stable isotope composition. It is suggested that the gradual reduction in the ²H and ¹⁸O content of precipitation in the study region, progressing from $\delta^{18}\text{O}$ values close to zero down to ca. -10‰ in the course of ISM evolution, stems from regional, large-scale recycling of moisture-driven monsoonal circulation. Superimposed on this general trend are short-term fluctuations of the isotopic composition of rainfall, which might have stem from local effects such as enhanced convective activity and the associated higher degree of rainout of moist air masses (local amount effect), the partial evaporation of raindrops, or the impact of isotopically heavy moisture generated in evapotranspiration processes taking place in the vicinity of rainfall sampling sites. Seasonal footprint maps constructed for

three stations representing the western, central and eastern portions of the Himalayan region indicate that the influence of monsoonal circulation reaches the western edges of the Himalayan region. While the characteristic imprint of monsoonal air masses (increase of monthly rainfall amount) can be completely absent in the western Himalayas, the onset of the ISM period in this region is still clearly visible in the isotopic composition of daily precipitation. A characteristic feature of daily precipitation collected during the WD period is the gradual increase of ²H and ¹⁸O content, reaching positive $\delta^{2}\text{H}$ and $\delta^{18}\text{O}$ values towards the end of the period. This trend can be explained by the growing importance of moisture of continental origin as a source of daily precipitation. High deuterium-excess (*d*-excess) values of daily rainfall recorded at the monitoring stations (38 cases in total, range from 20.6 to 44.0‰) are attributed to moisture of continental origin released into the atmosphere during the evaporation of surface water bodies and/or soil water evaporation.

1 Introduction

The Himalayas are a 2900 km long, west–northwest to east–southeast trending mountain range, which began to form between 40 and 50 Ma ago due to the collision of two large landmasses, India and Eurasia. This immense mountain range shapes the climate of southeast Asia and the Northern Hemisphere (e.g. Clemens et al., 1991; Molnar et al., 2010). The regional climate of the Himalayas is dominated by two

distinct circulation regimes of the regional atmosphere: the Indian summer monsoon (ISM) and the western disturbances (WD) periods.

The ISM is one of the most energetic components of the Earth's climate system, which develops in response to the movement of Intertropical Convergence Zone (ITCZ) that separates the atmospheric circulation of the northern and southern hemispheres (e.g. Gadgil, 2003; Allen and Armstrong, 2012). The warming of the Tibetan Plateau relative to the Indian Ocean, which results in low pressure over Asia and higher pressure over the Indian Ocean (Overpeck et al., 1996), pulls moisture from Southeast Asia and the Bay of Bengal and transports it north-westward (Hren et al., 2009; Li et al., 2016). There is an east–west gradient in monsoonal influence across the Himalayas with the central Himalayas receiving up to 80 % of its annual precipitation during the monsoon months according to some estimates (Bookhagen and Burbank, 2010; Lang and Barros, 2004).

Western disturbances are eastward moving synoptic low-pressure systems embedded in the lower to mid-tropospheric westerlies in the subtropics and originate from the Mediterranean Sea or mid-West Atlantic Ocean (Dimri et al., 2004, 2015; Maharana and Dimri, 2014; Madhura et al., 2015; Rao and Srinivasan, 1969; Pisharoty and Desai, 1956). At times, secondary systems of winds with embedded troughs develop over the Persian Gulf and the Black Sea either directly or as a result of the arrival of low-pressure systems from southwest Arabia (Dimri et al., 2004). Western disturbances cause heavy precipitation (>50 % of annual precipitation in winter) in the western Himalayas (Lang and Barros, 2004) and northern India from December to April (Pisharoty and Desai, 1956; Mooley, 1957; Agnihotri and Singh, 1982). They are also found to be active during the summer months, but with low frequency (Dhar et al., 1984; Dimri, 2006). When the troughs in the mid-tropospheric westerlies extend southwards into lower latitudes, the WD reach Afghanistan, Pakistan and India and are intensified by the moisture drawn from the Arabian Sea (Chand and Singh, 2015). Cannon et al. (2015) have shown that the heavy precipitation events occurring in the western and central Himalayas due to WD are spatiotemporally independent. The strength and frequency of WD over the last three decades (1979–2010) has increased in western Himalayas and decreased in the central Himalayas. On the basis of the variation in the deuterium-excess (d -excess) values of Ganges River water at Rishikesh, it was suggested that a significant fraction of the snow-melt and ice-melt components are derived from winter precipitation with a moisture source from the mid-latitude westerlies (Maurya et al., 2011). The impact of climate change on the frequency and magnitude of precipitation events in the tropics is still a matter of debate (Held and Soden, 2006; Wentz et al., 2007; Allan and Soden, 2008). This may be partly due to an inadequate understanding of the atmospheric water vapour dynamics (IPCC, 2013).

The flow of the Himalayan rivers, a key source of fresh water to more than a billion people (Ives and Messerli, 1989), primarily depends upon the strength, behaviour and duration of the WD and ISM. The rivers support one of the most heavily irrigated regions in the world (Tiwari et al., 2009) and are also critical for hydropower generation, the backbone of the region's economy (Karim and Veizer, 2002; Archer et al., 2010; Jeelani et al., 2012). Abnormal precipitation brought by WD and the ISM can lead to flooding or drought, which affects regional economies. Therefore, it is important to study spatiotemporal variability of the ISM and the WD in the Himalayas and to better characterize their causes and consequences. This implies, among others, a better understanding of the sources of atmospheric moisture forming precipitation in the region during the two contrasting circulation regimes of the lower atmosphere.

The stable isotope composition of oxygen and hydrogen in water molecules is a powerful tool for studies of the hydrological cycle, both with respect to its present status and its past behaviour. In the modern environment, the isotopic composition of precipitation serves as a conservative tracer for the origin, phase transitions and transport pathways of water (e.g. Dansgaard, 1964; Rozanski et al., 1993; Gat, 1996; Araguas-Araguas et al., 2000). The ^{18}O and ^2H content in precipitation are controlled by the following: (i) atmospheric parameters such as temperature, degree of rainout of the moist air masses and the amount of rainfall (e.g. Dansgaard, 1964; Yurtsever and Gat, 1981; Rozanski et al., 1982, 1993); and (ii) geographic factors such as altitude, latitude, moisture sources and atmospheric transport processes (e.g. Craig, 1961; Siegenthaler and Oeschger, 1980; Gat, 1996; Kendall and Coplen, 2001; Karim and Veizer, 2002). The $\delta^2\text{H}$ and $\delta^{18}\text{O}$ values in precipitation are tightly correlated and form a so-called global meteoric water line (GMWL) in the $\delta^2\text{H}$ – $\delta^{18}\text{O}$ space, defined by the following relationship: $\delta^2\text{H} = 8 \cdot \delta^{18}\text{O} + 10$ (Craig, 1963). A secondary isotope parameter, deuterium excess ($d = \delta^2\text{H} - 8 \cdot \delta^{18}\text{O}$; Dansgaard, 1964) defines the position of data points in the $\delta^2\text{H}$ – $\delta^{18}\text{O}$ space with respect to GMWL. The isotopic patterns of precipitation in the tropics are expected to be different from the sub-tropics and temperate regions due to large-scale convection systems, cyclonic storms and a multitude of vapour sources (e.g. Midhun et al., 2013; Lekshmy et al., 2014, 2015). Consequently, the well-established isotope effects such as the amount effect, the temperature effect and the altitude effect are not clearly visible in the precipitation isotope data sets available for the Indian subcontinent (Jeelani and Deshpande, 2017; Deshpande and Gupta, 2012; Deshpande et al., 2010; Warriar et al., 2010; Yavada, 2007). However, at local or watershed scales, stable water isotopes of precipitation showed a good relationship with altitude and temperature (Jeelani et al., 2017a, 2015, 2013; Kumar et al., 2010). The abrupt change in stable water isotopic values and the d -excess of precipitation during summer has been attributed to the reversal/change in the source of precipitation

from western disturbances to southwest monsoons (Jeelani et al., 2017b; Breitenbach et al., 2010).

The present study was launched with three major objectives: (i) to assess the seasonal variability of $\delta^{18}\text{O}$ and $\delta^2\text{H}$ in daily precipitation along the southern foothills of the Himalayas, (ii) to identify dominant moisture sources for precipitation in this region and (iii) to demarcate the influence of the Indian summer monsoon and western disturbances in the study area.

2 Study area

Daily precipitation samples were collected at six stations located along southern foothills of the Himalayas (Fig. 1 and Table 1). The stations cover a distance of almost 2900 km, from Srinagar in the west (Kashmir state) to Dibrugarh in the east (Assam state). In total, 548 daily precipitation samples were collected and analysed. The largest numbers of samples were available for Jorhat (242) and Srinagar (121) stations. The stations are open to the Indian subcontinent from the south and shielded by the Himalayan massif from the north. The elevation of the stations ranges from 99 (Jorhat) to 1872 m a.s.l. (Ranichauri). The mean annual temperature varies from 13.6 (Srinagar) to 24.2 °C (Jammu) and the mean annual precipitation ranges from 693 mm at Srinagar to 2781 mm at Dibrugarh.

Figure 2 shows long-term (1985–2014) monthly surface air temperature and precipitation data for the six stations where daily precipitation samples were collected. The data shown in Fig. 2 were grouped into two periods (Table 2): (i) Indian summer monsoons and (ii) western disturbances. The onset and duration of ISM periods were defined operationally on the basis of the seasonal distribution of long-term monthly rainfall, and through the examination of individual backward trajectories calculated for daily rainfall data gathered in the framework of the present study (cf. Sect. 4.1). The durations of ISMs varied from 3 months (July–September) for the stations located at the western edge (Srinagar, Jammu, Palampur) to 5 months (May–September) for the stations located at the eastern edge of the transect (Jorhat, Dibrugarh). For the central part of the transect (stations Ranichauri and Kathmandu) the onset of the ISM was set at the beginning of June and the termination at the end of September. For all stations except Srinagar station, the onset of the ISM is marked by a distinct increase in the monthly rainfall amount (cf. Fig. 2). For Srinagar station the rainfall imprint of the ISM onset and duration was not present; however, it could still be defined on the basis of backward trajectory analyses of the air masses associated with daily rainfall at this site, as well as through the characteristic ^{18}O and ^2H isotope signatures of this rainfall.

Long-term mean values of surface air temperature and cumulative precipitation, calculated for ISM and WD periods, are reported in Table 2 for stations where daily pre-

cipitation samples for isotope analyses were collected in the framework of this study. Also, the peak-to-peak amplitude of seasonal changes of monthly air temperature is reported. This amplitude increases gradually from the eastern (Dibrugarh: 11.7 °C) to the western edge of the transect (Srinagar: 23.1 °C), indicating progressive transition from a maritime to a continental climate. The mean temperatures for the ISM and WD periods also differ, the former being significantly higher; the average difference is approximately 8 °C.

The stations not only differ with respect to annual amount of rainfall (Table 1) but also with respect to cumulative rainfall amounts for ISM and WD periods, the former being generally higher (Table 2). The striking exception is Srinagar station – here the amount of rainfall during the WD period is significantly higher (543 mm) than that during the ISM period (150 mm). The ratio of cumulative rainfall amount during ISM and WD periods (parameter R in Table 2) varies from 3.41 for Dibrugarh to 1.95 for Ranichauri. For Srinagar, the value of this parameter is significantly lower than 1 (0.28).

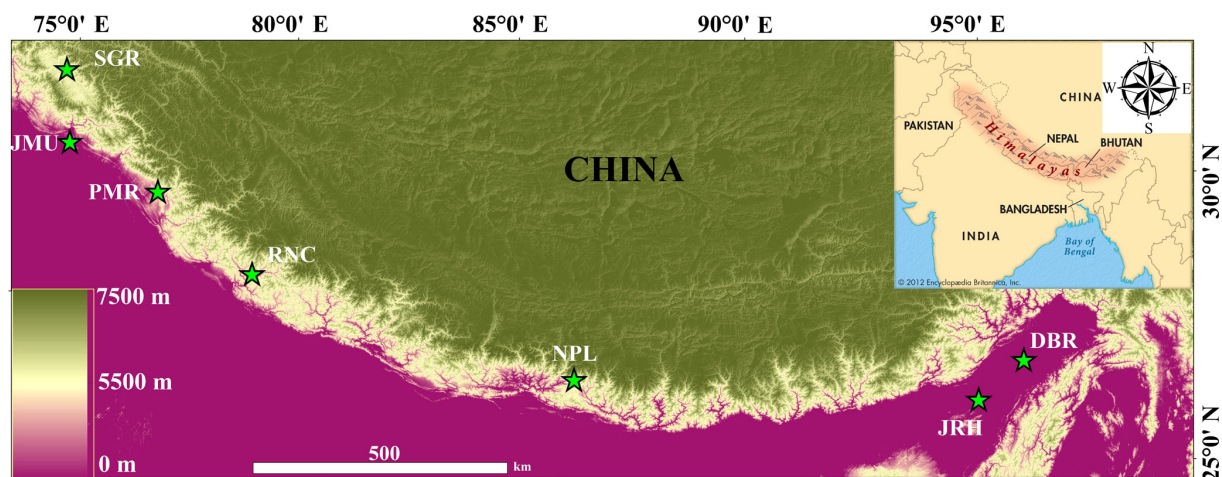
3 Methods

The Central Research Institute for Dryland Agriculture (CRIDA) and India Meteorological Department (IMD) collected most of the precipitation samples under the aegis of the “National Program on Isotope Fingerprinting of Waters of India” (IWIN) (Deshpande and Gupta, 2008, 2012). The India Meteorological Department, New Delhi, provided relevant meteorological data for the stations from its sub-offices. Deuterium and ^{18}O isotope composition of the rainfall samples were analysed using the IWIN-IRMS facility at the Physical Research Laboratory (PRL) Ahmadabad, following the standard equilibration method in which water samples were equilibrated with CO_2 (or H_2) and the equilibrated CO_2 (or H_2) gas was analysed by a Delta V Plus isotope ratio mass spectrometer (IRMS) in continuous flow mode using a Gasbench II preparation and introduction system (Maurya et al., 2009). The analytical uncertainty of the isotope analyses (one sigma) was ± 1.0 and ± 0.1 ‰ for $\delta^2\text{H}$ and $\delta^{18}\text{O}$, respectively.

The reconstruction of backward trajectories of the air masses arriving at the sampling stations was done through the framework of the Hybrid Single-Particle Lagrangian Integrated Trajectory model (HYSPPLIT4, revision February 2016 – Stein et al., 2015). The model was driven by the archived Global Data Assimilation System (GDAS1 product, available at <ftp://arlftp.arl.hq.noaa.gov/pub/archives/gdas1>, last access: March 2016) meteorological data available for every 3 h at $1.0^\circ \times 1.0^\circ$ horizontal resolution (corresponding to approx. 100 km \times 100 km), with 23 sigma pressure layers between 1000 and 20 hPa (Parrish and Derber, 1992). All trajectories were calculated with a temporal resolution of 30 min. For each location, the trajectory release

Table 1. General characteristics of the stations collecting daily precipitation samples for isotope analyses.

Station code	Station name	Latitude/Longitude	Altitude (m a.s.l.)	Mean annual temperature (°C)	Mean annual precipitation (mm)	Sampling period	Analysed rainfall events
SGR	Srinagar	34°04'59" N/ 74°47'50" E	1595	13.6	693	April 2010 to September 2011	121
JMU	Jammu	32°39'22" N/ 74°48'04" E	267	24.2	1238	July 2009 to June 2011	98
PMR	Palampur	32°06'01" N/ 76°32'49" E	1275	19.1	2493	September 2008 to September 2010	31
RNC	Ranichauri	30°18'50" N/ 78°24'25" E	1872	15.1	1272	February 2009 to December 2010	31
JRH	Jorhat	26°43'21" N/ 94°11'44" E	99	24.0	2324	February 2010 to December 2011	242
DBR	Dibrugarh	27°29'05" N/ 95°01'18" E	111	23.2	2781	June 2009 to October 2010	25

**Figure 1.** Locations of the six sampling sites across the southern foothills of the Himalayas: SGR – Srinagar, JMU – Jammu, PMR – Palampur, RNC – Ranichauri, JRH – Jorhat and DBR – Dibrugarh. The position of the Kathmandu station, Nepal (NPL), which is discussed in the text, is also marked in the figure.

point was set up at 500 m above the local ground level in order to represent mean elevation of moist air masses.

Ten-day backward trajectories representing daily rainfall samples were calculated as trajectory ensembles, each consisting of twenty seven ensemble members released at 12:00 LT on the day of precipitation sample collection. Ensembles were produced by varying the initial trajectory wind speeds and pressures, according to the HYSPLIT ensemble algorithm, in order to account for the uncertainties involved in the simulation of individual backward trajectories. A slight modification of the default algorithm was used, with the horizontal range of sampling of the initial values reduced from a 1 to a 0.5 grid cell width in the driving meteorological field. As no information about exact timing of precipitation events

(except of the date) was available, the question of representativity of the backward trajectories released at 12:00 LT was investigated in some detail. For selected events multiple releases (every three hours) were realized for the given day. The results did not reveal any significant changes in ensemble patterns, neither in terms of trajectory source areas nor in the behaviour of the presented meteorological variables. Apparently, the ensemble scheme largely captured the variability of the transport patterns associated with generation of rainfall events sampled at the stations.

For footprint analysis, individual 10-day backward trajectories starting from 12:00 LT were calculated for each station collecting daily rainfall and for Kathmandu station, Nepal, which represented the central region of the transect. Daily

Table 2. Long-term (1985–2014) characteristics of surface air temperature and precipitation for Indian summer monsoon (ISM) and western disturbances (WD) periods, for the stations collecting daily precipitation samples for isotope analyses. Source of data: Srinagar, Jammu, Palampur, Jorhat and Dibrugarh – <https://pl.climate-data.org/> (last access: April 2016); Ranichauri – Upadhyay et al. (2015).

Station	^a Duration of ISM	^b A_T (°C)	ISM period		WD period		^c R
			T (°C)	P (mm)	T (°C)	P (mm)	
Srinagar	July–September	23.1	23.0	150	10.5	543	0.28
Jammu	July–September	21.0	29.7	854	22.4	384	2.22
Palampur	July–September	17.2	23.2	1772	15.6	721	2.46
Ranichauri	June–September	14.4	20.5	842	12.4	431	1.95
Jorhat	May–September	12.3	28.1	1759	21.0	565	3.11
Dibrugarh	May–September	11.7	27.1	2151	20.5	630	3.41

^a Onset and duration of ISM period defined operationally on the basis of seasonal distribution of long-term monthly rainfall (cf. Fig. 2) and through examination of individual backward trajectories calculated for daily rainfall events collected by each station in the framework of the present study.

^b Peak-to-peak amplitude of long-term (1985–2014) seasonal changes of monthly surface air temperature at the station.

^c The ratio of cumulative rainfall amount collected at the given station during ISM and WD periods.

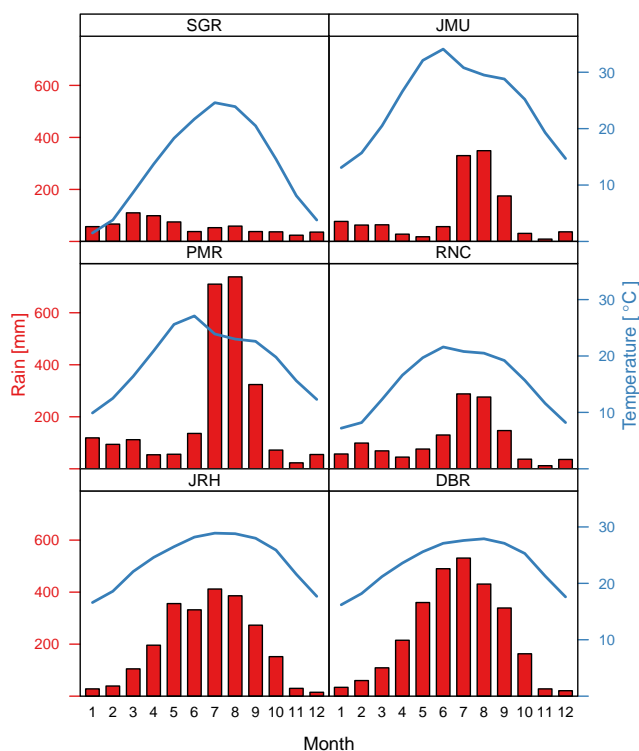


Figure 2. Long-term (1985–2014) monthly surface air temperature and precipitation data for six stations where daily sampling of rainfall for isotope analyses was conducted. SGR – Srinagar, JMU – Jammu, PMR – Palampur, RNC – Ranichauri, JRH – Jorhat and DBR – Dibrugarh. Source of data: Srinagar, Jammu, Palampur, Jorhat and Dibrugarh – <https://pl.climate-data.org/>; Ranichauri – Upadhyay et al. (2015).

releases over the course of three consecutive years (2009–2011) were simulated. The chosen period corresponds with

the period of precipitation sampling at the stations. Daily trajectories calculated over the three-year period were then aggregated to produce the footprint maps. Footprints representative of the ISM and WD seasons were calculated using the subsets of available trajectories. The output was a $0.5^\circ \times 0.5^\circ$ footprint signal, which was later smoothed spatially using the focal averaging method.

4 Results and Discussion

4.1 Seasonality of isotope characteristics of daily rainfall

Figure 3 shows seasonal changes of $\delta^{18}\text{O}$ and deuterium excess for the two stations with the largest number of daily isotope data available (Jorhat – 242 data points, and Srinagar – 121 data points). These two stations are located on the western (Srinagar) and eastern (Jorhat) edges of the study transect (cf. Fig. 1). They have been selected to illustrate the seasonal evolution of the isotopic composition of daily precipitation at the stations along the east–west study transect. Figure S1 in the Supplement summarizes $\delta^{18}\text{O}$ and deuterium excess records available for other four stations. The ^{18}O isotope composition of daily precipitation at Jorhat and Srinagar stations shown in Fig. 3a reveals a distinct seasonality, particularly well displayed in the data available for Jorhat station. During development of the Indian summer monsoon, the ^{18}O content in daily precipitation at this site gradually decreases, from $\delta^{18}\text{O}$ values fluctuating around 0‰ at the onset of ISM, to very negative $\delta^{18}\text{O}$ values (up to ca. -20‰) recorded at its termination. During the WD period the ^{18}O content progressively increases, reaching positive δ values towards the end of the period. The seasonality of the ^{18}O signal is also well marked at other stations (Fig. S1a). As suggested by Fig. 3a, the largest heavy isotope depletion in rainfall is expected at the transition from the ISM to the WD period. In-

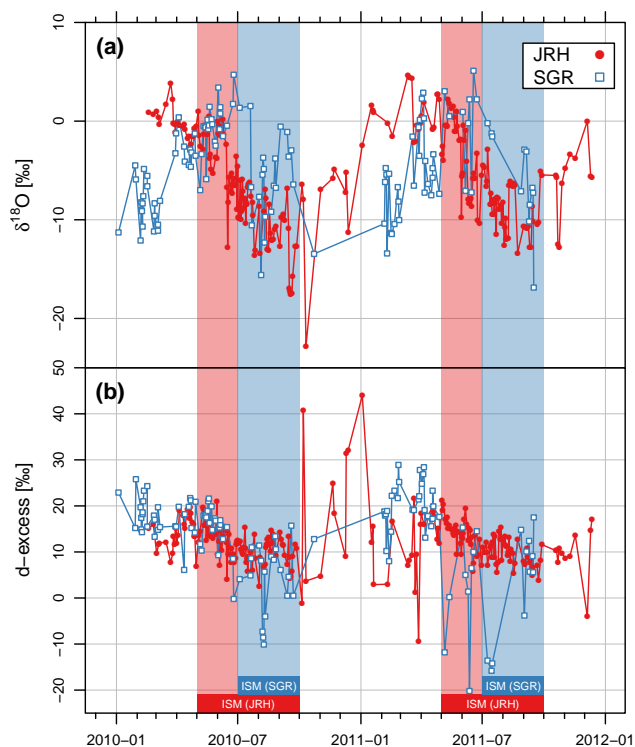


Figure 3. Seasonal variations of $\delta^{18}\text{O}$ (a) and d -excess (b) of daily rainfall collected at the Jorhat (JRH) and Srinagar (SGR) stations. The Indian summer monsoon (ISM) period at Srinagar (July–September) and Jorhat (May–September) is marked in blue and red shading, respectively.

deed, the three most negative $\delta^{18}\text{O}$ values of daily rainfall recorded during this study (Ranichauri: -19.48‰ , Jorhat: -22.79‰) were observed in September and October. Conversely, the most positive $\delta^{18}\text{O}$ values (Jammu: $+8.20$ and $+9.28\text{‰}$) were observed towards the end of the WD period (April, June). Although d -excess records shown in Fig. 3b are rather noisy, it is apparent that the d -excess progressively decreases at Srinagar site from high d -excess values recorded in January–February ($d > 20\text{‰}$) to low d -excess values ($d < 10\text{‰}$) recorded in September. At Jorhat, temporal evolution of the d -excess values largely coincides with the trend observed at Srinagar. However, during the WD period, the d -excess is much more variable at Jorhat and ranges from 0 to more than 40‰ .

Negative values of the d -excess were recorded from time to time at all stations along the transect (35 events in total, cf. Figs. 3 and S1b). An extreme value (-28.8‰) was recorded at Palampur station in February 2010 and was associated with very light rain ($< 1\text{ mm}$). As seen in Figs. 3 and S1b, the largest number of events characterized by negative d -excess values was recorded at Jammu station (19 in total). Such events predominantly occurred at this site during the WD period (17 out of 19 registered cases). Nega-

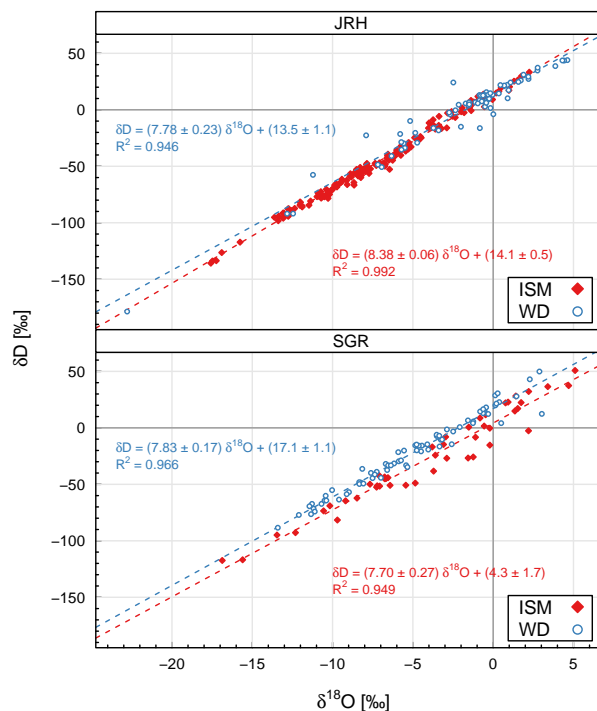


Figure 4. $\delta^2\text{H}$ – $\delta^{18}\text{O}$ relationship for daily isotope data available for Jorhat (JRH) and Srinagar (SGR) stations. Local meteoric water lines were calculated separately for Indian summer monsoon (ISM) and western disturbances (WD) periods.

tive d -excess values were also observed during the western African monsoon (Risi et al., 2008; Landais et al., 2010) and were generally attributed to the re-evaporation of raindrops. Raindrops falling through unsaturated atmosphere below the cloud-base level undergo partial evaporation. This process was investigated in the laboratory by Steward (1975) and was modelled (e.g. Bony et al., 2008). The relative magnitude of ^2H and ^{18}O fractionation effects associated with the evaporation process cause the evaporating water droplet to become enriched in heavy isotopes and evolve in the $\delta^2\text{H}$ – $\delta^{18}\text{O}$ space along the line with a slope significantly lower than eight (e.g. Rozanski et al., 2001). Thus, evaporating raindrops will move away from the local meteoric water line (LMWL), eventually reaching negative d -excess values. The extent of partial evaporation is mainly controlled by the relative humidity of the atmosphere through which raindrops are falling as well as by the isotopic composition of ambient moisture. In fact, the WD period at Jammu station is characterized by an exceptionally low relative humidity (average value for WD period ca. 35%) when compared to other stations. This may explain the large number of rainfall events with negative d -excess values recorded at this station.

Figure 4 shows daily $\delta^2\text{H}$ and $\delta^{18}\text{O}$ data available for Srinagar and Jorhat stations, grouped into ISM and WD periods and plotted on a $\delta^2\text{H}$ – $\delta^{18}\text{O}$ graph. Analogous plots for other stations are presented in the Supplement (Fig. S2). During the monsoon season the linear relationship between $\delta^2\text{H}$ and $\delta^{18}\text{O}$ is generally better defined, pointing to moisture sources of a similar nature and similar rainfall formation conditions. At the Srinagar site, there is a striking difference between local meteoric water lines representing the ISM and WD periods. The intercept of the LMWL representing the ISM is more than two times lower than the LMWL representing the WD period, with both lines displaying similar slopes. A similar situation is observed for Ranichauri station. For Jorhat and Dibrugarh the seasonal differences in the LMWL are less pronounced. Local meteoric water lines representing the WD period for Jammu and Palampur stations have significantly lower slopes (5.8 and 5.5, respectively) pointing to the importance of the re-evaporation of raindrops at these sites outside of the monsoon season (Fig. S2).

The summary isotope statistics of daily rainfall data available for all six stations, grouped into ISM and WD periods, are presented in Table 3. Arithmetic averages of three isotope parameters characterizing daily rainfall ($\delta^2\text{H}$, $\delta^{18}\text{O}$, d -excess) with their respective uncertainties were calculated for both periods. Arithmetic averaging was chosen in order to better reflect average conditions at moisture sources and in the regional atmosphere during the considered periods. The $\delta^{18}\text{O}$ values of daily precipitation were correlated with the daily surface air temperature and rainfall amount available for each station. Linear correlations were calculated separately for ISM and WD periods. The last two columns of Table 3 summarize those calculations. Box and whisker plots of daily $\delta^{18}\text{O}$ and d -excess data available for each station and season are summarized in Fig. 5.

As seen in Table 3 and Fig. 5, ISM and WD periods are characterized by distinct isotope signatures of precipitation collected along the southern foothills of the Himalayas. Average $\delta^2\text{H}$ and $\delta^{18}\text{O}$ values for the ISM period are significantly lower than those recorded for the WD period at the given station. The largest difference (ca. 7.5‰ for $\delta^{18}\text{O}$ and 60‰ for $\delta^2\text{H}$) was observed at Palampur station. Rainfall collected during ISM and WD periods also differs with regards to the mean d -excess values. During ISM, d values are generally lower than those observed during the WD period. In one case (Jammu station) this regularity is broken (very low mean d -excess for WD period). This anomalously low mean d -excess stems from the fact that a large proportion of rainfall events exhibit negative d -excess values (cf. discussion above). There is a lack of distinct spatial trends in the mean isotope characteristics of daily rainfall along the study transect during the two seasons (cf. Fig. 5). As far as the link between $\delta^{18}\text{O}$ and local surface air temperature is concerned, positive, significant correlations were found for three stations: Srinagar (ISM period), Jammu (both periods) and Ranichauri (WD period). Significant negative correla-

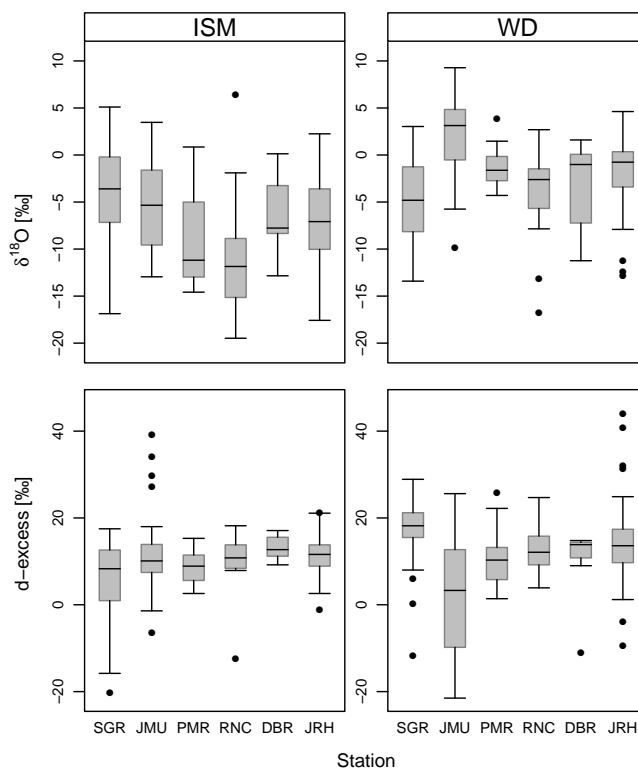


Figure 5. Box and whisker plots for $\delta^{18}\text{O}$ and d -excess values of daily rainfall at the six stations (Srinagar – SGR; Jammu – JMU; Palampur – PMR; Ranichauri – RNC; Jorhat – JRH; and Dibrugarh – DBR) collecting daily rainfall samples along southern foothills of the Himalayas (cf. Fig. 1). The data are grouped into Indian summer monsoon (ISM) and western disturbances (WD) periods.

tions were observed for Jorhat and Dibrugarh stations (ISM period).

Distinct seasonality seen in the isotope characteristics of daily rainfall at the southern foothills of the Himalayas should be viewed in the context of large-scale seasonal changes in the circulation regime of the regional atmosphere. These changes can be best illustrated through the reconstruction of back trajectories of moist air masses generating rainfall events at selected sites of the east–west transect. Backward trajectory modelling was performed for all daily precipitation events analysed in the framework of this study (548 events). Figures 6 and 7 show examples of typical backward trajectories (ensembles) representing ISM and WD periods, reconstructed for Jorhat and Srinagar stations, and representative of the eastern and western edges of the transect, respectively. The lower panels of Figs. 6 and 7 show the evolution of selected parameters of the air parcels transported along the trajectories: (i) elevation above the local ground (m), (ii) terrain height (m a.s.l.), (iii) velocity of the air parcel (m s^{-1}), (iv) temperature of the air parcel ($^{\circ}\text{C}$), (v) precipitation rate (mm per 6 h) and (vi) H_2O mixing ratio (g kg^{-1}).

Table 3. Mean isotope characteristics of daily precipitation collected at the six stations along southern foothills of the Himalayas, calculated for the Indian summer monsoon (ISM) and western disturbances (WD) periods. Slopes of the best fit lines approximating the relationship between surface air temperature ($\Delta\delta^{18}\text{O} / \Delta T$) and precipitation amount ($\Delta\delta^{18}\text{O} / \Delta P$), based on daily data available for each period, are reported in the last two columns of the table.

Station	^a Period	$\delta^{18}\text{O}$ (‰)	$\delta^2\text{H}$ (‰)	<i>d</i> -excess (‰)	^b <i>N</i>	^c ($\Delta\delta^{18}\text{O} / \Delta T$)	^c ($\Delta\delta^{18}\text{O} / \Delta P$)
Srinagar	ISM	-5.81 ± 0.79	-42.6 ± 5.8	3.9 ± 1.6	31	+	±
	WD	-4.19 ± 0.48	-17.2 ± 3.7	16.3 ± 0.8	90	±	–
Jammu	ISM	-5.34 ± 0.63	-30.9 ± 4.6	11.5 ± 1.1	51	+	±
	WD	1.94 ± 0.58	17.3 ± 3.6	1.8 ± 1.8	47	+	±
Palampur	ISM	-8.70 ± 2.51	-60.9 ± 17.6	8.7 ± 2.5	12	±	±
	WD	-1.24 ± 0.28	-0.7 ± 0.2	11.3 ± 1.4	19	±	±
Ranichauri	ISM	-8.96 ± 2.11	-60.8 ± 14.3	10.8 ± 2.5	18	±	±
	WD	-2.16 ± 0.58	-4.1 ± 1.1	13.2 ± 3.5	13	+	±
Jorhat	ISM	-6.88 ± 0.52	-43.3 ± 3.3	11.7 ± 0.9	172	±	±
	WD	-1.99 ± 0.24	-2.2 ± 0.3	13.8 ± 1.6	70	–	±
Dibrugarh	ISM	-6.64 ± 1.65	-40.2 ± 10.1	12.9 ± 3.2	16	–	n.d.
	WD	-1.92 ± 0.64	-4.5 ± 1.5	10.9 ± 3.6	9	±	n.d.

^a Onset and duration of the Indian summer monsoon (ISM) period defined operationally on the basis of the seasonal distribution of long-term monthly rainfall (cf. Fig. 2) and thorough examination of individual backward trajectories calculated for daily rainfall data collected by each station in the framework of the present study. Duration of the ISM for Srinagar, Jammu and Palampur: July–September; for Ranichauri: June–September; for Jorhat and Dibrugarh: May–September. The rest of the year is defined as western disturbances (WD).

^b Number of daily precipitation samples analysed.

^c “+” signifies a positive, significant ($R \geq 0.4$) correlation between $\delta^{18}\text{O}$ and daily temperature or precipitation. “–” signifies a negative, significant ($R \geq 0.4$) correlation between $\delta^{18}\text{O}$ and daily temperature or precipitation. “±” signifies the lack of a significant ($R \geq 0.4$) correlation between $\delta^{18}\text{O}$ and daily temperature or precipitation. “n.d.” signifies “not determined”.

The ISM period at Jorhat station (Fig. 6a) is dominated by the low-level transport of moist air masses (water vapour content of ca. 18 g kg^{-1}) from the equatorial Indian Ocean and the Bay of Bengal. The calculated ensembles have relatively low spread, reflecting the large-scale, uniform movement of the moist air masses driven by monsoon circulation. The air masses reach the station from the south, without any noticeable contribution from other directions. Rainfall is generated when warm, moist air masses are lifted up over the continent and cool down from ca. 28 to 20°C . As seen in Fig. 7a, the monsoonal air masses may reach also the Srinagar station located on the western edge of the transect. However, the ensembles shown in Fig. 7a suggest that the more direct route of moist monsoonal air masses (water vapour content of ca. 15 g kg^{-1}), starting in the Arabian Sea and crossing the Indian continent, is a more important source of rainfall for western Himalayas during this season than trajectories passing over the Bay of Bengal and travelling along the southern foothills of the Himalayas in the northwest direction. During WD period, the overwhelming majority of air masses arrive at rainfall collection stations from the west and northwest (Figs. 6b and 7b). Typically, they travel at high elevations (4000 – 6000 m a.g.l.), passing the Black Sea and Caspian Sea regions, and further descend over Afghanistan and Pakistan, towards the rainfall collection stations located at the western edge of the transect (Srinagar, Jammu, Palampur). These dry air masses (water vapour content around 1 g kg^{-1}) pick

up moisture of continental origin from relative proximity to the collection sites and their vapour content rises to approx. 3.5 g kg^{-1} (Fig. 7b – lower panel). For stations located at the eastern edge of the transect (Jorhat, Dibrugarh) more western routes of air masses prevail (Fig. 6b). Air masses travel east within the latitude band of 20 to 30° N passing the Arabian Peninsula, the Persian Gulf, the northern reaches of the Arabian Sea and northern India, gradually warming up and losing elevation. On their way east they gradually absorb moisture of both marine (Arabian Sea) and continental origin. As a result of this process, their water vapour content rises from approximately 3 g kg^{-1} at the eastern coast of the Arabian Peninsula to ca. 8 g kg^{-1} in the proximity of the eastern edge of the transect.

4.2 Evolution of $\delta^{18}\text{O}$ during ISM period

The gradual, heavy isotope depletion of rainfall in the course of the development and recession of the Indian summer monsoon, as apparent from Figs. 3a and S1, is not a local phenomenon only restricted to the study transect. Such evolution of $\delta^{18}\text{O}$ in precipitation is observed over the entire region influenced by the ISM. For instance, $\delta^{18}\text{O}$ of monthly rainfall at New Delhi decreases from ca. 0‰ in June to around -9‰ in September (Araguas et al., 1998; Battacharya et al., 2003). The IWIN programme stations (Deshpande and Gupta, 2008, 2012) also show a similar trend with the grad-

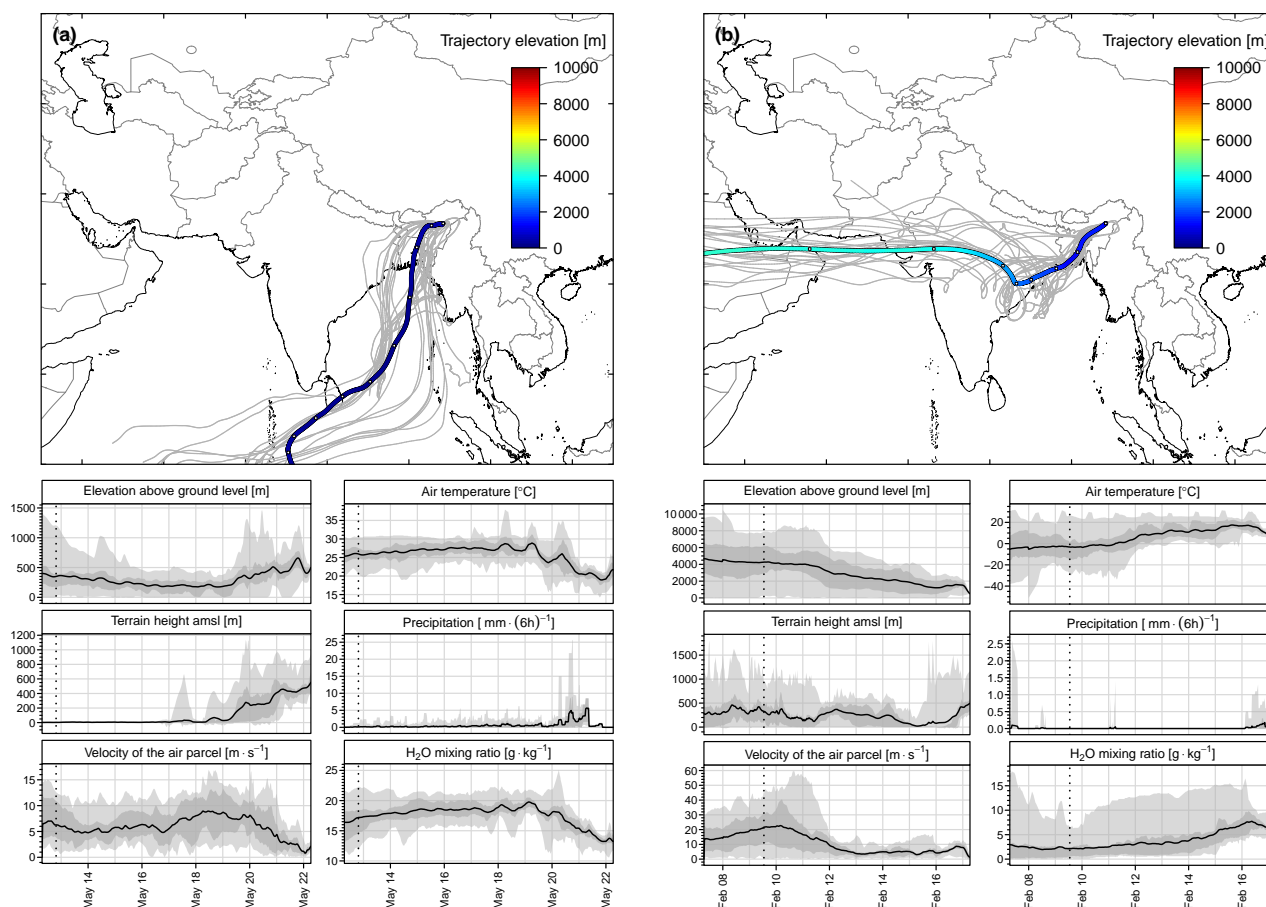


Figure 6. (a) Upper diagram: 10-day backward trajectories arriving at Jorhat station on 22 May 2010, 12:00 LT and representing the Indian summer monsoon (ISM) period. (b) Upper diagram: 10-day backward trajectories arriving at Jorhat station on 17 February 2011, 12:00 LT and representing the western disturbances (WD) period. Twenty seven ensembles (grey lines in the background) and the mean trajectory (heavy line) are shown. The colours of the mean trajectory indicate elevation above ground level in metres. Empty white dots on the mean trajectory indicate 24 h intervals. Lower diagrams of (a) and (b) show the evolution of the six selected parameters of the air parcel along the trajectory. Evolution of the mean value of each parameter is marked with a heavy black line and the associated uncertainty in grey. Dashed vertical lines mark the part of the mean 10-day trajectory visible in the upper diagram. International boundaries are only indicative and as provided by the software.

ual decrease of $\delta^{18}\text{O}$ values of rainfall towards the end of the ISM season in September, e.g. Ahmedabad station in western India (Deshpande et al., 2010). A reduction of the ^{18}O content of similar magnitude was observed for individual rainfall events collected during the 2012 and 2013 monsoon period on Andaman Island, in the Bay of Bengal (Chakraborty et al., 2016).

The extent of heavy isotope depletion of daily rainfall in the course of the ISM evolution, observed in this study, is large ($> 10\text{‰}$ in $\delta^{18}\text{O}$). Regional thermal gradients are virtually non-existent during ISM; hence, they cannot be used to explain the observed gradual reduction of $\delta^{18}\text{O}$, with sea surface temperatures in the Bay of Bengal fluctuating between 28 and 29 °C (e.g. Midhun et al., 2013) and mean surface air temperatures at three low-elevation stations of the study transect (Jammu, Jorhat, Dibrugarh) around 28 °C (cf. Ta-

ble 2). This gradual reduction of heavy isotope content in precipitation is apparently a regional phenomenon inherently linked to the evolution of the Indian summer monsoon and cannot be explained by local effects. Local effects such as enhanced convective activity in the local atmosphere and the associated higher degree of rainout of moist air masses (local amount effect) or partial evaporation of raindrops, might explain the short-term fluctuations of $\delta^{18}\text{O}$ visible in Figs. 3a and S1a; however, local effects will not explain the regional evolution of $\delta^{18}\text{O}$ and $\delta^2\text{H}$ values over the course of the ISM. Clearly, another explanation should be considered here. In this context, it is noteworthy that Deshpande et al. (2015) have shown that major moisture uptake locations for precipitation at Ahmedabad gradually change from over the Arabian Sea to central Indian continental areas in the later part of the ISM.

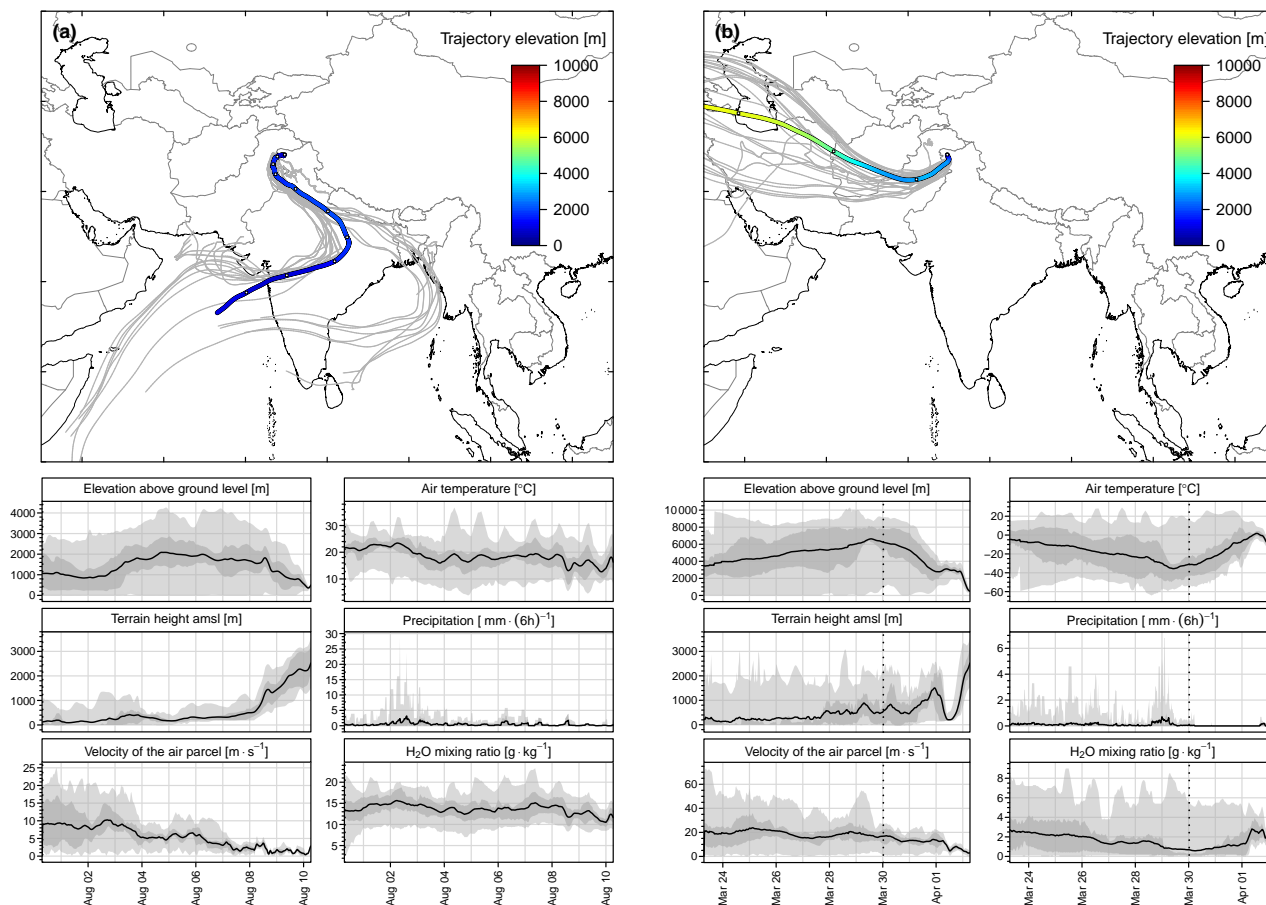


Figure 7. (a) Upper diagram: 10-day backward trajectories arriving at Srinagar station on 10 August 2010, 12:00 LT and representing the Indian summer monsoon (ISM) period. (b) Upper diagram: 10-day backward trajectories arriving at Srinagar station on 2 April 2011, 12:00 LT and representing the western disturbances (WD) period. Twenty seven ensembles (grey lines in the background) and the mean trajectory (heavy line) are shown. The colours of the mean trajectory indicate the elevation above ground level in metres. Empty white dots on the mean trajectory indicate 24 hour intervals. The lower panels of (a) and (b) show the evolution of the six selected parameters of the air parcel along the trajectory. The evolution of the mean value of each parameter is marked by a heavy black line and the associated uncertainty in grey. Dashed vertical lines represent the part of the mean 10-day trajectory visible in the upper diagram. International boundaries are only indicative and as provided by the software.

Over the course of the ISM period, water availability from surface (lakes, reservoirs, streams, wetlands) and sub-surface (soil, vadose zone) environments and in the lower atmosphere over large continental areas of India progressively increases to a substantial extent. For instance, in the state of Assam 9.7 % of the region is under wetlands including rivers, streams and riverine wetlands during this period. The open pan annual evaporation (2.36 mm day^{-1}) and annual potential evapotranspiration (3 mm day^{-1}) at Jorhat is the lowest in the country (Rao et al., 2012). The relative humidity is generally higher during the summer months from June to November. The low values of open pan and potential evapotranspiration and high relative humidity in Assam suggest that the atmosphere remains continuously loaded with locally generated moisture during the summer months. As the monsoon progresses in India, enhanced soil moisture and vegetation

cover lead to increased evapotranspiration and recycled precipitation. The recycling ratio, which is the ratio of recycled precipitation to total precipitation, is highest (around 25 %) in northeast India, where dense vegetation cover leads to high evapotranspiration. A high precipitation recycling ratio was found at the end of the monsoon in the month of September (Pathak et al., 2014).

The increasing amount of moisture in the lower atmosphere over the course of the ISM makes the air column unstable and prone to convective activities. It should be noted here that in the absence of horizontal thermal gradients between source regions of atmospheric moisture and the continent, the principal mechanisms which can generate rainfall are vertical uplift and the cooling of moist air masses, which are associated with convective systems. If the horizontal and vertical extent of convective systems increase as the monsoon

progresses, they could generate the observed gradual depletion of heavy isotopes in daily rainfall over the course of the ISM evolution.

Looking from a broader perspective, a large-scale, regional recycling of moisture of oceanic origin can also contribute to the observed evolution of $\delta^{18}\text{O}$ and $\delta^2\text{H}$ during the ISM period. Northward movement of the ITCZ pulls maritime moisture from Southeast Asia and the Bay of Bengal and transports it north-westward. Moist air masses are lifted by large-scale convection, lose part of their moisture content and return towards the equator as the upper branch of Hadley cell circulation. Then, they descend and mix with the low-level moist air masses of oceanic origin (cf. Li et al., 2016 – Fig. 24). Descending air masses contain moisture depleted of heavy isotopes, which is then incorporated in the moist air masses of oceanic origin transported north-westward. A regional recycling loop such as this, operating in the course of ISM evolution, may provide the required mechanism for a gradual, large-scale reduction of the ^{18}O and ^2H content in regional atmospheric moisture and precipitation during this period. A rough assessment of this effect was made assuming a Rayleigh-type rainout of moist air masses of oceanic origin ($\text{RH} = 80\%$, $T = 28^\circ\text{C}$), with the initial $\delta^{18}\text{O}$ value of moisture equal to -10% . It was assumed that rainout induced by large-scale convection continues down to 15% of the initial water content. Dry air masses containing vapour depleted in heavy isotopes return as an upper branch of the recycling loop and mix with the moist air masses of oceanic origin. Five to six such recycling loops would be required to reduce the initial ^{18}O content of maritime moisture and the rainfall by approximately 10% at the end of the monsoon period, in accordance with observations.

It is likely that both of the mechanisms underlined above act together to produce the observed characteristic evolution of $\delta^{18}\text{O}$ and $\delta^2\text{H}$ in daily rainfall during the ISM period. Model runs of isotope general circulation models available for Indian continent (e.g. Hoffman and Heimann, 1997; Midhun and Ramesh, 2016) suggest that the models tend to underestimate the amplitude of seasonal changes of $\delta^{18}\text{O}$, particularly in northern India. A more comprehensive isotope modelling of monsoon circulation would be needed to quantify the above-outlined mechanisms of moisture recycling and their impact on the measured stable isotope composition of precipitation in the region.

Finally, worth commenting on, are the large seasonal changes in the isotopic composition of regional atmospheric moisture reservoir in response to the contrasting circulation patterns of the regional atmosphere and moisture recycling mechanisms discussed above. When the operation of the monsoon circulation engine is terminated in September, the regional atmosphere is still loaded with moisture heavily depleted in ^2H and ^{18}O . This remarkable heavy isotope depletion of the regional atmospheric moisture reservoir survives for several weeks. In fact, the most negative $\delta^{18}\text{O}$ value (-22.79%) was measured in rainfall collected at Jorhat sta-

tion on 11 October 2010. In the course of the WD period, maritime moisture depleted in heavy isotopes is gradually replaced by moisture of continental origin characterized by elevated concentration of ^2H and ^{18}O (cf. discussion below). This, in turn, is reflected in rising δ values of rainfall over the course of the WD period.

4.3 Positive $\delta^{18}\text{O}$ and $\delta^2\text{H}$ values of daily rainfall

A striking feature of the isotope data generated in the framework of this study is the relatively frequent appearance of positive $\delta^{18}\text{O}$ and $\delta^2\text{H}$ values in the isotope records available for six stations collecting daily rainfall. Positive δ values range from 0.17 to 9.28‰ for $\delta^{18}\text{O}$ and from 5.3 to 56.6‰ for $\delta^2\text{H}$. They constitute ca. 16% of the collected and analysed data. Positive $\delta^{18}\text{O}$ and $\delta^2\text{H}$ values were mostly recorded during the WD period (ca. 25% of all data available for this period, compared to 5.5% recorded during the ISM period). The station where positive $\delta^{18}\text{O}$ and $\delta^2\text{H}$ values were recorded most frequently (70% of the data available for the WD period) was Jammu. To better characterize rainfall events showing positive δ values, d -excess values calculated for such events were plotted as a function of (positive) $\delta^{18}\text{O}$ values and the relative humidity of the local atmosphere (daily means). The resulting plots are shown in Fig. 8. As seen in Fig. 8, d -excess values decrease with increasing $\delta^{18}\text{O}$ values ($R^2 = 0.349$) and increase with rising relative humidity (RH) of the local atmosphere ($R^2 = 0.147$). In a comprehensive study of the western African monsoon precipitation near Niamey (Niger) (Landais et al., 2010), a significantly higher slope of d -excess–RH correlation was found (0.38) compared to that characterizing data points shown in the lower panel of Fig. 8 (0.22 ± 0.05). Also the variables were much better correlated ($R^2 = 0.68$, Fig. 7b in Landais et al., 2010). However, this is not surprising, keeping in mind that the data reported by Landais et al. (2010) originated from one station (Banbizoumbou) and were restricted to the monsoon season (June–September). Conversely, the data shown in Fig. 8 covered both seasons (ISM and WD) and represented six stations distributed along a 2900 km transect of the southern foothills of the Himalayas. Moreover, relative humidity data in the Landais et al. (2010) study were reconstructed mean RH values for the lower troposphere (200–1000 m a.g.l.), whereas this study used daily means of RH values measured near ground level.

The ^{18}O isotope composition of maritime moisture, collected onboard a ship (mast top, ca. 25 m a.s.l.) cruising the Bay of Bengal during the ISM period (from 13 July to 3 August 2012), varied between ca. -10 and -14% (Midhun et al., 2013). If one adopts -10% as a representative $\delta^{18}\text{O}$ value for unaltered oceanic moisture from which monsoon precipitation is formed, and further assumes that this moisture is transported towards the southern foothills of the Himalayas without any noticeable rainout effect, the expected $\delta^{18}\text{O}$ value of the first condensate would be around -1.0% .

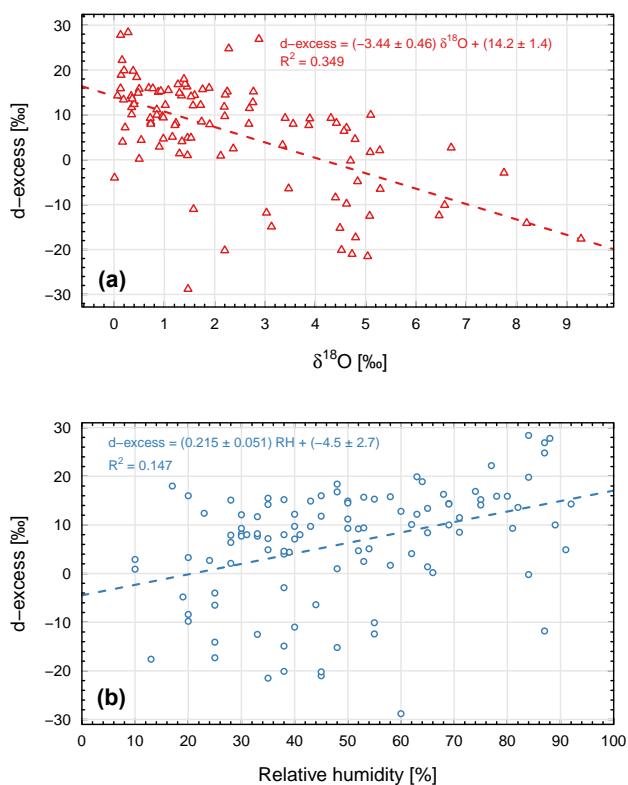


Figure 8. (a) The relationship between deuterium excess and positive $\delta^{18}\text{O}$ values measured in daily precipitation samples collected at six stations distributed along the southern foothills of the Himalayas (cf. Fig. 1). (b) The relationship between deuterium excess and relative humidity of the local, near-ground atmosphere (daily means) calculated for precipitation events exhibiting positive $\delta^{18}\text{O}$ values.

However, it is highly unlikely that unaltered maritime moisture can reach remote continental sites such as Jammu station, where positive δ values are most common. Hence, the “first condensate” scenario cannot fully explain the positive $\delta^{18}\text{O}$ and $\delta^2\text{H}$ values recorded at the stations along the transect, even if the partial evaporation of raindrops on their way to the ground is considered.

As the majority of the positive δ values was recorded during the WD period, the explanation of positive $\delta^{18}\text{O}$ and $\delta^2\text{H}$ values should involve sources of moisture other than oceanic ones. One can distinguish three components of the backward flux of water into the regional atmosphere over the continental areas, each characterized by distinct isotope signature: (i) water transpired by plant cover, (ii) water evaporated from bare soil and (iii) water evaporated from surface water bodies. It is a well-established fact that in the course of the transpiration process, leaf water becomes progressively enriched in heavy stable isotopes, quickly reaching hydrologic and isotopic steady state (e.g. Dongmann et al., 1974; Flanagan et al., 1991). Under such conditions, the

isotopic composition of water vapour released into the atmosphere is isotopically identical to the source water utilized by plants. In our case the water utilized by plants predominantly originates from the rainy (monsoon) season. The amount-weighted mean $\delta^{18}\text{O}$ of ISM precipitation for three low-altitude stations (Jammu, Dibrugarh, Jorhat) is -6.5‰ . First condensate produced from such water vapour (assumed condensation temperature of $+10^\circ\text{C}$) will be characterized by $\delta^{18}\text{O}$ values close to $+4.2\text{‰}$, which fall within the range of positive δ values of daily rainfall collected at the stations. Soil water evaporation may also produce water vapour, the isotopic composition of which is identical to that of the source (soil) water. However, due to the much larger size of the soil water reservoir compared to leaf water, establishing a steady-state isotope evaporation profile in the soil column requires much longer periods of time than is the case for the leaf water reservoir (weeks instead of hours). This is only possible under arid or semi-arid conditions, where periods between consecutive rain events are long enough (e.g. Zimmerman et al., 1966; Barnes et al., 1983) which is generally not the case for the study area. Evaporation from bare soil in this case will resemble evaporation from open water bodies. The isotopic composition of evaporating surface water bodies evolve in the $\delta^2\text{H}-\delta^{18}\text{O}$ space along the so-called local evaporation line with the slope significantly lower than eight (e.g. Gat, 1996). The mass balance considerations require that water vapour being released into the local atmosphere in the course of such process is located on the local evaporation line, to the left-hand side of the local meteoric water line (LMWL). This water vapour has a somewhat reduced heavy isotope content when compared to the source water subject to evaporation and is characterized by high deuterium excess (e.g. Rozanski et al., 2001).

All three processes outlined above are most probably acting together under climatic conditions characteristic of the study region. These processes are also apparently capable of delivering sufficient amounts of moisture to the regional atmosphere to produce rainfall characterized by positive δ values, even at locations which are far away from oceanic sources of water. It is likely that generally higher and more variable d -excess values of rainfall events recorded in the course of the WD period (cf. Figs. 3a and S1a), reflect the varying contribution of those three processes to the backward flux of moisture into the regional atmosphere, generated by the Indian subcontinent during that time of the year. The fact that d -excess values are inversely correlated with $\delta^{18}\text{O}$ and increase with the rising relative humidity of the near-ground atmosphere (cf. Fig. 8), point to the partial evaporation of raindrops as an additional mechanism contributing to the observed range of positive $\delta^{18}\text{O}$ and $\delta^2\text{H}$ values.

4.4 Significance of elevated d -excess values

A higher than the global average d -excess value (ca. 10‰) in meteoric waters originating from the Himalayas and Ti-

betan Plateau was often used to infer Mediterranean or more generally westerly derived vapour (Tian et al., 2005; Hren et al., 2009; Jeelani et al., 2010; Bershaw et al., 2012). The observed high d -excess in rainfall was generally related to the higher d -excess (ca. 20‰) found in the vapour generated over eastern Mediterranean Sea (Gat and Carmi, 1970). Here we argue that these high d -excess values recorded in the Himalayas do not necessarily originate from the Mediterranean Sea. There were 38 rainfall events with $d > 20$ ‰ observed in this study (ca. 6.9 % of all events analysed). Higher d -excess values mostly occurred during the WD period (31 out of 38 cases). However, the highest d values were recorded during the ISM period (Jammu, 34.0 and 39.1‰; Jorhat, 40.7 and 44.0‰).

The largest number of events characterized by high d -excess values was recorded at Srinagar station during the WD period (21 out of 90 analysed for this period). The only station without elevated d -excess values was Dibrugarh. Closer examination of backward trajectory ensembles calculated for days with high d -excess values reveal that trajectories associated with daily rainfall samples characterized by high d -excess values arrive at Srinagar from the northwest, west or southwest. However, as discussed above, these air masses are generally very dry and only pick-up moisture of continental origin in relative proximity to rainfall collection stations (cf. Fig. 7b). Surprisingly, high d -excess values recorded at Jammu station are almost exclusively associated with characteristic monsoon-type circulation (Fig. S3). In one case, recorded during the WD period (31 December 2010), the air masses were circling around over the Indian subcontinent and interacting strongly with the surface.

A common feature of almost all trajectories at all the precipitation sites with high d -excess is their long residence time in relative proximity of the sampling site, as illustrated in Fig. S4 for Jorhat station. This long residence time leaves enough time for their prolonged interaction with the surface, during which evaporation of surface water bodies (lakes, swamps, etc.) and/or non-steady-state evaporation of soil moisture serve as important sources of water vapour characterized by high d -excess values. Rainfall produced from such vapour will retain this characteristic isotope signature in the form of a high d -excess value. Some impact of atmospheric moisture with high d -excess arriving from the eastern Mediterranean in the Himalayan region is certainly possible, although in our opinion it is rather unlikely that this is an important source of rainfall in the region. Low-level eastward moving, turbulent transport of moisture from the eastern Mediterranean towards the Himalayas will inevitably be associated with strong interaction with the surface on the way (rainfall, backward moisture fluxes) which will blur the original isotope signature of the moisture of marine origin.

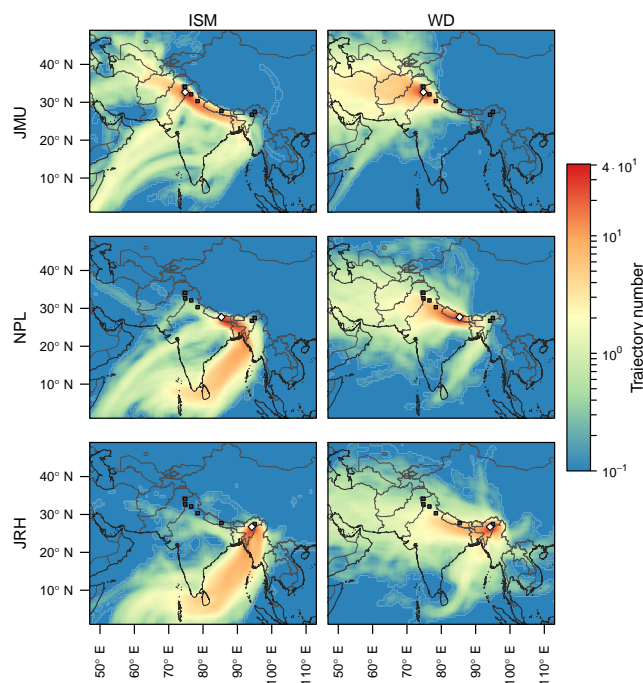


Figure 9. Footprint maps of air masses arriving at three stations: Jammu (JMU), Kathmandu (NPL) and Jorhat (JRH) representing the respective western, central and eastern parts of the east–west study transect along southern foothills of the Himalayas (a, b, c). Separate maps were prepared for the Indian summer monsoon (ISM) and western disturbances (WD) periods. Daily trajectories for the period 2009–2011 were reconstructed using the HYSPLIT modelling framework (see text for details). International boundaries are only indicative and as provided by the software. The colour scale indicates the focally averaged number of trajectories passing through a grid cell.

4.5 Footprint analysis

To better characterize the contribution of different air masses arriving in the course of ISM and WD seasons, at the six stations collecting daily rainfall along southern foothills of the Himalayas, footprint analysis was performed. Footprint maps were calculated for the 2009–2011 period, based on daily simulations of 10-day long backward trajectories, starting at each of the locations at noon local time. Footprint maps were prepared for three stations (Jammu, Kathmandu and Jorhat) representing the western, central and eastern parts of the study transect, respectively. Separate maps were constructed for ISM and WD periods and are presented in Fig. 9. The maps shown in Fig. 9 provide valuable insight into the great seasonal contrast in the circulation patterns of the regional atmosphere, which in turn control the rainfall regime in the region (amount, seasonal distribution and stable isotope composition).

The footprint map representing the ISM period at Jorhat station clearly demonstrates the overwhelming dominance of

the monsoon circulation bringing moisture-loaded air masses from the tropical Indian Ocean and the Bay of Bengal towards the eastern region of the Himalayas. There is a very small contribution (in the order of few percent) from the air masses arriving from the west and northwest. The dominating influence of monsoon air masses is also seen in the central portion of the transect (Kathmandu site), although the presence of air masses originating in the Arabian Sea and crossing Indian subcontinent in the northeast direction is also noticeable. The footprint map for Jammu station representing the western Himalayas clearly shows three major types of air masses arriving at this site during the ISM period: (i) maritime monsoonal air masses originating in the Bay of Bengal and travelling along southern foothills of the Himalayas, (ii) continental air masses coming from the northwest and (iii) air masses originating in the Arabian Sea and travelling along the India–Pakistan border towards eastern Himalayas; the first of these being the dominating component.

During the WD period, the circulation patterns of the regional atmosphere change radically. The Jorhat station receives air masses predominantly from northern India and Pakistan, with a noticeable contribution from the Bay of Bengal. The footprint map is generally more diffuse, indicating the presence of continental air masses with an origin in central Asia as well as the Black Sea and Caspian Sea regions. A similar occurrence is observed at Kathmandu station, with majority of air masses coming from northern India and Pakistan. The impact of maritime air masses (Bay of Bengal) is reduced, although it is still visible. The western part of the Himalayas (Jammu station) is under the overwhelming influence of air masses coming from the west (Iran, Iraq, Afghanistan and Pakistan). While the small contribution of oceanic air masses coming from the eastern Arabian Sea is still visible, air masses coming from the Bay of Bengal are practically absent.

5 Conclusions

Isotope analyses of daily precipitation samples collected at six stations located along the southern foothills of the Himalayas allowed a deeper insight into the mechanisms controlling the isotopic composition of precipitation in this important region of the Indian subcontinent. The analysis of the ^2H and ^{18}O isotope composition of daily precipitation, combined with extensive backward trajectory modelling of the air masses associated with rainfall in the study region, allowed several important conclusions to be drawn with respect to origin of atmospheric moisture and precipitation in two contrasting seasons (Indian summer monsoon and western disturbances).

It is suggested that the gradual reduction in the ^2H and ^{18}O content of precipitation in the region, progressing from positive $\delta^{18}\text{O}$ values, down to less than -10‰ in the course of ISM evolution, stems from convective activities in the re-

gional atmosphere and large-scale recycling of moisture of oceanic origin, driven by monsoonal circulation. Superimposed on this general trend are short-term fluctuations of the isotopic composition of rainfall which may stem from local effects such as locally enhanced convective activity and the associated higher degree of rainout of moist air masses (local amount effect), partial evaporation of raindrops, or the impact of isotopically heavy moisture generated in evapotranspiration processes taking place in the vicinity of rainfall sampling sites. Seasonal footprint maps constructed for three stations representing the western, central and eastern portions of the Himalayan region indicate that the influence of monsoonal circulation reaches the western edges of the Himalayan region. While the characteristic imprint of monsoon air masses (increase of monthly rainfall amount) can be completely absent in the eastern Himalayas, the onset of the ISM period is still clearly visible in the isotopic composition of individual precipitation events.

The most characteristic feature of daily precipitation collected in the study region during the WD period is its relatively high ^2H and ^{18}O content when compared to the ISM period, and the presence of a large number of daily rainfall samples exhibiting positive $\delta^{18}\text{O}$ and $\delta^2\text{H}$ values. These peculiar isotope characteristics can only be explained when a continental origin of the source moisture for this precipitation is postulated. Water stored in the soil during the ISM period is returned to the regional atmosphere during the WD period through the evapotranspiration processes. Backward trajectory modelling has shown that long-range transport of air masses from the west and northwest, characteristic of the WD period, occurs at high elevations and cannot bring sufficient amounts of moisture to significantly contribute to precipitation in the study area during this period. Instead, the major supply of moisture for rainfall during the WD period is mainly of local (regional) origin, stemming from the transpiration of plant cover, soil water evaporation and the evaporation of surface water bodies. All of these processes deliver water vapour which is significantly enriched in heavy isotopes compared to unaltered vapour of oceanic origin. This enrichment is then reflected in the isotopic composition of rainfall produced from such vapour. Isotope characteristics of rainfall during the WD period are consistent with this scenario. Seasonal footprint maps show that during this period eastward moving air masses may reach the eastern edges of the Himalayas. Footprint maps also suggest the presence of air masses coming from the Bay of Bengal, which bring moisture of oceanic origin to the study area, cannot be excluded.

It appears that high d -excess values of daily rainfall collected along southern foothills of the Himalayas can be associated with air masses of very different origins. However, the common feature of almost all air masses is their relatively long interaction with the continental surface, which provides a chance to accommodate enough moisture of continental

origin; this moisture is characterized by elevated d -excess values, which then is transferred to the local rainfall.

Data availability. All the isotope data used in this manuscript can be requested from Rajendrakumar D. Deshpande at desh@prl.res.in. Backward trajectory modelling was done for all daily precipitation events analysed in the framework of this study. The modelling results as well as the data used to construct footprint maps are available on request from Michal Galkowski (Michal.Galkowski@fis.agh.edu.pl).

Supplement. The supplement related to this article is available online at: <https://doi.org/10.5194/acp-18-8789-2018-supplement>.

Author contributions. GJ drafted the manuscript with input from RDD, MG and KR. All the authors reviewed the manuscript and interpreted the data. MG conducted the HYSPLIT modelling.

Competing interests. The authors declare that they have no conflict of interest.

Acknowledgements. Parts of the sampling and the isotope analyses discussed in this study were undertaken under the aegis of the IWIN National Programme (Deshpande and Gupta, 2008) jointly funded by the Department of Science and Technology (DST), Govt. of India, vide Grant No. IR/ S4/ESF-05/2004 and the Physical Research Laboratory (PRL). Authors acknowledge support from DST and PRL with gratitude. The IMD and CRIDA collected rainwater samples from some of the stations included in this study. Michal Galkowski and Kazimierz Rozanski were supported by the statutory funds of the AGH University of Science and Technology (project no. 11.11.220.01/1). We appreciate the constructive comments from one anonymous reviewer and Michael Schulz, co-editor of ACP. They helped us to considerably improve the manuscript.

Edited by: Michael Schulz

Reviewed by: Michael Schulz and one anonymous referee

References

- Agnihotri, C. L. and Singh, M. S.: Satellite study of western disturbances, *Mausam*, 33, 249–254, 1982.
- Allan, R. P. and Soden, B. J.: Atmospheric warming and the amplification of precipitation extremes, *Science*, 321, 1481–1484, 2008.
- Allen, M. B. and Armstrong, H. A.: Reconciling the Intertropical Convergence Zone, Himalayan/Tibetan tectonics, and the onset of the Asian monsoon system, *J. Asian Earth Sci.*, 44, 36–47, 2012.
- Araguás-Araguás, L., Froehlich, K., and Rozanski, K.: Stable isotope composition of precipitation over Southeast Asia, *J. Geophys. Res.*, 103, 28721–28742, 1998.
- Araguás-Araguás, L., Froehlich, K., and Rozanski, K.: Deuterium and oxygen-18 isotope composition of precipitation and atmospheric moisture, *Hydrol. Process.*, 14, 1341–1355, 2000.
- Archer, D. R., Forsythe, N., Fowler, H. J., and Shah, S. M.: Sustainability of water resources management in the Indus Basin under changing climatic and socio economic conditions, *Hydrol. Earth Syst. Sci.*, 14, 1669–1680, <https://doi.org/10.5194/hess-14-1669-2010>, 2010.
- Barnes, C. J. and Allison, G. B.: The distribution of deuterium and O-18 in dry soils, 1. Theory, *J. Hydrol.*, 60, 141–156, 1983.
- Bershaw, J., Penny, S. M., and Garzzone, C. N.: Stable isotopes of modern water across the Himalaya and eastern Tibetan Plateau: Implications for estimates of paleoelevation and paleoclimate, *J. Geophys. Res.-Atmos.*, 117D2, <https://doi.org/10.1029/2011JD016132>, 2012.
- Bhattacharya, S. K., Froehlich, K., Aggarwal, P. K., and Kulkarni, K. M.: Isotopic variation in Indian Monsoon precipitation: records from Bombay and New Delhi, *Geophys. Res. Lett.*, 30, 2285, <https://doi.org/10.1029/2003GL018453>, 2003.
- Bony, S., Rissi, C., and Vimeux, F.: Influence of convective processes on the isotopic composition ($\delta^{18}\text{O}$ and δD) of precipitation and water vapour in the tropics: 1. Radiative-convective equilibrium and Tropical Ocean-Global Atmosphere-Coupled Ocean-Atmosphere Response Experiment (TOGA-COARE) simulations, *J. Geophys. Res.*, 113, D19305, <https://doi.org/10.1029/2008JD009942>, 2008.
- Bookhagen, B. and Burbank, D. W.: Toward a complete Himalayan hydrological budget: spatiotemporal distribution of snowmelt and rainfall and their impact on river discharge, *J. Geophys. Res.*, 115, F03019, <https://doi.org/10.1029/2009JF001426>, 2010.
- Breitenbach, S. F. M., Adkins, J. F., Meyer, H., Marwan, N., Kumar, K. K., and Haug, G. H.: Strong influence of water vapour source dynamics on stable isotopes in precipitation observed in southern Meghalaya, NE India, *Earth Planet. Sc. Lett.*, 292, 212–220, 2010.
- Cannon, F., Carvalho, L. M. V., Jones, C., and Bookhagen, B.: Multi-annual variations in winter westerly disturbance activity affecting the Himalaya, *Clim. Dynam.*, 44, 441–455, 2015.
- Chakraborty, S., Sinha, N., Chattopadhyay, R., Sengupta, S., Mohan, P. M., and Datye, A.: Atmospheric controls on the precipitation isotopes over the Andaman Islands, Bay of Bengal, *Sci. Rep.*, 6, 19555, <https://doi.org/10.1038/srep19555>, 2016.
- Chand, R. and Singh, C.: Movement of Western Disturbances and associated cloud convection, *J. Ind. Geophys. Union*, 19, 62–70, 2015.
- Clemens, S., Prell, W., Murray, D., Shimmield, G., and Weedon, G.: Forcing mechanisms of the Indian Ocean monsoon, *Nature*, 353, 720–725, 1991.
- Craig, H.: Isotope variations in meteoric waters, *Science*, 133, 1702–1703, 1961.
- Dansgaard, W.: Stable isotopes in precipitation, *Tellus*, 16, 436–468, 1964.
- Deshpande, R. D. and Gupta, S. K.: National programme on isotope fingerprinting of waters of India (IWIN), *Glimpses of Geosciences Research in India, the Indian Report to IUGS, Indian National Science Academy*, 10–16, 2008.

- Deshpande, R. D. and Gupta, S. K.: Oxygen and hydrogen isotopes in hydrological cycle: New data from IWIN national programme, *P. Indian Nat. Acad. Sci.*, 78, 321–331, 2012.
- Deshpande, R. D., Maurya, A. S., Kumar, B., Sarkar, A., and Gupta, S. K.: Rain-vapor interaction and vapor source identification using stable isotopes from semi-arid Western India, *J. Geophys. Res.*, 115, D23311, <https://doi.org/10.1029/2010JD014458>, 2010.
- Deshpande, R. D., Dave, M., Padhya, V., Kumar, H., and Gupta, S. K.: Water vapour source identification for daily rain events at Ahmedabad in semi-arid western India: wind trajectory analyses, *Meteorol. Appl.*, 22, 754–762, 2015.
- Dhar, O. N., Kulkarni, A. K., and Sangam, E. B.: Some aspects of winter & monsoon rainfall distribution over the Garhwal-Kumaon Himalaya: a brief appraisal, *Himal. Res. Dev.*, 2, 10–19, 1984.
- Dimri, A. P.: Surface and upper air fields during extreme winter precipitation over the western Himalayas, *Pure Appl. Geophys.*, 163, 1679–1698, 2006.
- Dimri, A. P., Mohanty, U. C., and Mandal, M.: Simulation of heavy precipitation associated with an intense western disturbance over Western Himalayas, *Nat. Hazards*, 31, 499–521, 2004.
- Dimri, A. P., Niyogi, D., Barros, A. P., Ridley, J., Mohanty, U. C., Yasunari, T., and Sikka, D. R.: Western Disturbances: A review, *Rev. Geophys.*, 53, 225–246, 2015.
- Dongmann, G., Nurnberg, H. W., Förstel, H., and Wagener, K.: On the enrichment of $H_2^{18}O$ in the leaves of transpiring plants, *Radiat. Environ. Bioph.*, 11, 41–52, 1974.
- Flanagan, L. B., Marshall, J. D., and Ehleringer, J. R.: Comparison of modelled and observed environmental influences on the stable oxygen and hydrogen isotope composition of leaf water in *Phaseolus vulgaris* L, *Plant Physiol.*, 96, 623–631, 1991.
- Gadgil, S.: The Indian monsoon and its variability, *Annu. Rev. Earth Pl. Sc.*, 31, 429–467, 2003.
- Gat, J. R.: Oxygen and hydrogen isotopes in the hydrologic cycle, *An. Rev. Earth Planet. Sci.*, 24, 225–262, 1996.
- Gat, J. R. and Carmi, I.: Evolution of the isotopic composition of atmospheric waters in the Mediterranean Sea area, *J. Geophys. Res.*, 75, 3039–3048, 1970.
- Held, I. M. and Soden, B. J.: Robust response of the hydrological cycle to global warming, *J. Climate*, 19, 5686–5699, 2006.
- Hren, M. T., Bookhagen, B., Blisniuk, P. M., Booth, A. L., and Chamberlain, C. P.: $\delta^{18}O$ and δD of streamwater across Himalayan and Tibetan Plateau: Implications for moisture sources and palaelevation studies, *Earth Planet. Sci. Lett.*, 288, 20–32, 2009.
- Hoffmann, G. and Heimann, M.: Water isotope modelling in the Asian monsoon region, *Quatern. Int.*, 37, 115–128, 1997.
- IPCC: Climate Change 2013: The Physical Science Basis, Contribution of Working Group I to the Fifth Assessment Report of the Intergovernmental Panel on Climate Change, edited by: Stocker, T. F., Qin, D., Plattner, G.-K., Tignor, M., Allen, S. K., Boschung, J., Nauels, A., Xia, Y., Bex, V., and Midgley, P. M., Cambridge University Press, Cambridge, United Kingdom and New York, NY, USA, 1535 pp., <https://doi.org/10.1017/CBO9781107415324>, 2013.
- Ives, J. D. and Messerli, B.: The Himalayan Dilemma: Reconciling Development and Conservation, John Wiley, London, <https://doi.org/10.4324/9780203169193>, 1989.
- Jeelani, G. and Deshpande, R. D.: Isotope fingerprinting of precipitation associated with western disturbances and Indian summer monsoons across the Himalayas, *J. Earth Syst. Sci.*, 126, 108, <https://doi.org/10.1007/s12040-017-0894-z>, 2017.
- Jeelani, G., Bhat, N. A., and Shivanna, K.: Use of ^{18}O tracer to identify stream and spring origins of a mountainous catchment: a case study from Liddar watershed, Western Himalaya, India, *J. Hydrol.*, 393, 257–264, 2010.
- Jeelani, G., Faddema, J., Van der Veen, C., and Leigh, S.: Role of snow and glacier melt in controlling river hydrology in Liddar watershed (western Himalaya), *Water Resour. Res.*, 48, W12508, <https://doi.org/10.1029/2011WR011590>, 2012.
- Jeelani, G., Kumar, U. S., and Kumar, B.: Variation of $\delta^{18}O$ and δD in precipitation and stream waters across the Kashmir Himalaya (India) to distinguish and estimate the seasonal sources of stream flow, *J. Hydrol.*, 481, 157–165, 2013.
- Jeelani, G., Kumar, U. S., Bhat, N. A., Kumar, B., and Sharma, S.: Variation of $\delta^{18}O$, δD and 3H in karst springs of south Kashmir, western Himalayas (India), *Hydrol. Process.*, 29, 522–530, 2015.
- Jeelani, G., Shah, R. A., Deshpande, R. D., Fryer, A., Perrin, J., and Mukherjee, A.: Distinguishing and estimating recharge to karst springs in snow and glacier dominated mountainous basins of the western Himalaya, India, *J. Hydrol.*, 550, 239–252, 2017a.
- Jeelani, G., Deshpande, R. D., Shah, R. A., and Hassan, W.: Influence of southwest monsoons in Kashmir Valley, Western Himalaya, *Isot. Environ. Health, S.*, 53, 400–412, 2017b.
- Karim, A. and Veizer, J.: Water balance of the Indus River Basin and moisture source in the Karakoram and western Himalayas: Implications from hydrogen and oxygen isotopes in river water, *J. Geophys. Res.-Atmos.*, 107, 4362, <https://doi.org/10.1029/2000JD000253>, 2002.
- Kendall, C. and Coplen, T. B.: Distribution of oxygen-18 and deuterium in river waters across the United States, *Hydrol. Process.*, 15, 1363–1393, 2001.
- Kumar, B., Rai, S. P., Kumar, U. S., Verma, S. K., Garg, P., Kumar, S. V. V., Jaiswal, R., Purendra, B. K., Kumar, S. R., and Pande, N. G.: Isotopic characteristics of Indian precipitation, *Water Resour. Res.*, 46, 1–15, 2010.
- Landais, A., Rissi, C., Bony, S., Vimeux, F., Descroix, L., Falourd, S., and Bouygues, A.: Combined measurements of $^{17}O_{\text{excess}}$ and d -excess in African monsoon precipitation: Implications for evaluating convective parameterizations, *Earth Planet. Sci. Lett.*, 298, 104–112, 2010.
- Lang, T. J. and Barros, A. P.: Winter storms in the central Himalayas, *J. Meteor. Soc. Jpn.*, 82, 829–844, 2004.
- Lekshmy, P. R., Midhun, M., Ramesh, R., and Jani, R. A.: ^{18}O depletion in monsoon rain relates to large scale organized convection rather than the amount of rainfall, *Sci. Rep.*, 4, 5661, <https://doi.org/10.1038/srep05661>, 2014.
- Lekshmy, P. R., Midhun, M., and Ramesh, R.: Spatial variation of amount effect over peninsular India and Sri Lanka: role of seasonality, *Geophys. Res. Lett.*, 42, 5500–5507, <https://doi.org/10.1002/2015GL064517>, 2015.
- Li, Z., Lau, W. K.-M., Ramanathan, V., Wu, G., Ding, Y., Manoj, M. G., Liu, J., Qian, Y., Li, J., Zhou, T., Fan, J., Rosenfeld, D., Ming, Y., Wang, Y., Huang, J., Wang, B., Xu, X., Lee, S.-S., Cribb, M., Zhang, F., Yang, X., Zhao, Z., Takemura, T., Wang, K., Xia, X., Yin, Y., Zhang, H., Gou, J., Zhai, P. M., Sugimoto, N., Babu, S. S., and Brasseur, G. P.: Aerosol and mon-

- soon climate interactions in Asia, *Rev. Geophys.*, 54, 866–929, <https://doi.org/10.1002/2015RG000500>, 2016.
- Madhura, R. K., Krishnan, R., Revadekar, J. V., Mujumdar, M., and Goswami, B. N.: Changes in western disturbances over the Western Himalayas in a warming environment, *Clim. Dynam.*, 44, 1157–1168, 2015.
- Maharana, P. and Dimri, A. P.: Study of seasonal climatology and interannual variability over India and its sub-regions using a regional climate model (RegCM3), *Earth Sys. Sci.*, 123, 1147–1169, 2014.
- Maurya, A. S., Shah, M., Deshpande, R. D., and Gupta, S. K.: Protocol for $\delta^{18}\text{O}$ and δD analyses of water sample using Delta V plus IRMS in CF Mode with Gas Bench II for IWIN National Programme at PRL, Ahmedabad, Proceedings of the 11th ISMAS Triennial Conference of Indian Society for Mass Spectrometry, Hyderabad, Indian Society for Mass Spectrometry, Mumbai, 24–28 November, 2009, 314–317, 2009.
- Maurya, A. S., Shah, M., Deshpande, R. D., Bhardwaj, R. M., Prasad, A., and Gupta, S. K.: Hydrograph separation and precipitation source identification using stable water isotopes and conductivity: River Ganga at Himalayan foothills, *Hydrol. Process.*, 25, 1521–1530, 2011.
- Molnar, P., Boos, W. R., and Battisti, D. S.: Orographic controls on climate and paleoclimate of Asia: thermal and mechanical roles for the Tibetan Plateau, *An. Rev. Earth Planet. Sci.*, 38, 77, <https://doi.org/10.1146/annurev-earth-040809-152456>, 2010.
- Midhun, M. and Ramesh, R.: Validation of $\delta^{18}\text{O}$ as a proxy for past monsoon rain by multi-GCM simulations, *Clim. Dynam.*, 46, 1371–1385, 2016.
- Midhun, M., Lekshmy, P. R., and Ramesh, R.: Hydrogen and oxygen isotopic compositions of water vapor over the Bay of Bengal during monsoon, *Geophys. Res. Lett.*, 40, 6324–6328, 2013.
- Mooley, D. A.: The role of western disturbances in the production of weather over India during different seasons, *Ind. J. Meteorol. Geophys.*, 8, 253–260, 1957.
- Overpeck, J., Anderson, D., Trumbore, S., and Prell, W.: The southwest Indian Monsoon over the last 18 000 years, *Clim. Dynam.*, 12, 213–225, 1996.
- Parrish, D. F. and Derber, J. C.: The National Meteorological Center's Spectral Statistical-Interpolation Analysis System, *Mon. Weather Rev.*, 120, 1747–1763, [https://doi.org/10.1175/1520-0493\(1992\)120<1747:TNMCS>2.0.CO;2](https://doi.org/10.1175/1520-0493(1992)120<1747:TNMCS>2.0.CO;2), 1992.
- Pathak, A., Ghosh S., and Kumar, P.: Precipitation recycling in the Indian subcontinent during summer monsoon, *J. Hydromet.*, 15, 2050–2066, 2014.
- Pisharoty, P. R. and Desai, B. N.: Western disturbances and Indian weather, *Ind. J. Meteorol. Geophys.*, 8, 333–338, 1956.
- Rao, Y. P. and Srinivasan, V.: Forecasting Manual, Part II Discussion of typical synoptic weather situation: winter western disturbances and their associated features, *Ind. Meteorol. Depart., FMU, Report No. III-1*, 1969.
- Rao, B. B., Sandeep, V. M., Rao, V. U. M., and Venkateswarlu, B.: Potential evapotranspiration estimation for Indian conditions: Improving accuracy through calibration coefficients, *Tech. Bull.*, 1, 1–60, 2012.
- Risi, C., Bony, S., Vimeux, F., Descroix, L., Ibrahim, B., Lebreton, E., Mamadou, I., and Sultan, B.: What controls the isotopic composition of the African monsoon precipitation? Insights from event-based precipitation collected during the 2006 AMMA field campaign, *Geophys. Res. Lett.*, 35, L24808, <https://doi.org/10.1029/2008GL035920>, 2008.
- Rozanski, K., Sonntag, C., and Münnich, K. O.: Factors controlling stable isotope composition of European precipitation, *Tellus*, 34, 142–150, 1982.
- Rozanski, K., Araguás-Araguás, L., and Gonfiantini, R.: Isotopic patterns in modern global precipitation, in: *Climate Change in Continental Isotopic Records*, Geophysical Monograph 78, American Geophysical Union, Washington D.C., 1–36, 1993.
- Rozanski, K., Froehlich, K., and Mook, W. G.: Surface water, in: *Environmental Isotopes in the Hydrological Cycle*, Vol. III, Technical Documents in Hydrology, No. 39, UNESCO, IAEA, 117 pp., 2001.
- Siegenthaler, U. and Oeschger, H.: Correlation of ^{18}O in precipitation with temperature and altitude, *Nature*, 285, 314–317, 1980.
- Steward, M. K.: Stable isotope fractionation due to evaporation and isotopic exchange of falling waterdrops: applications to atmospheric processes and evaporation of lakes, *J. Geophys. Res.*, 80, 1133–1146, 1975.
- Stein, A. F., Draxler, R. R., Rolf, G. D., Stundler, B. J. B., Cohen, M. D., and Ngan, F.: NOAA's HYSPLIT atmospheric transport and dispersion modeling system, *B. Am. Meteorol. Soc.*, 96, 2059–2077, 2015.
- Tian, L., Tandong, Y., White, J. W. C., Wusheng, Y., and Ninglian, W.: Westerly moisture transport to the middle of Himalayas revealed from the high deuterium excess, *Chinese Sci. Bull.*, 50, 1026–1030, 2005.
- Tiwari, V. M., Wahr, J., and Swenson, S.: Dwindling groundwater resources in northern India from satellite gravity observations, *Geophys. Res. Lett.*, 36, L18401, <https://doi.org/10.1029/2009GL039401>, 2009.
- Upadhyay, R. G., Ranjan, R., and Negi, P. S.: Climatic variability and trend at Ranichauri (Uttarakhand), *J. Agrometeorol.*, 17, 241–243, 2015.
- Warrier, C. U., Babu, M. P., Manjula, P., Velayudhan, K. T., Hameed, S. A., and Vasu, K.: Isotopic characterization of dual monsoon precipitation: evidence from Kerala, India, *Curr. Sci.*, 98, 1487–1495, 2010.
- Wentz, F. J., Ricciardulli, L., and Hilburn, K.: How much more rain will global warming bring, *Science*, 317, 233–235, 2007.
- Yadava, M. G., Ramesh, R., and Pandarinath, K.: A positive amount effect in the Sahayadri (Western Ghats) rainfall, *Curr. Sci.*, 93, 560–564, 2007.
- Yurtsever, Y. and Gat, J.: Atmospheric waters, in: *Stable isotope hydrology: Deuterium and oxygen-18 in the water cycle*, edited by: Gat, J. R. and Gonfiantini, R., IAEA, Vienna, Austria, 103–142, 1981.
- Zimmermann, U., Ehhalt, D. H., and Münnich, K. O.: Soil water movement and evapotranspiration: changes in the isotopic composition of water, *Isotopes in Hydrology*, IAEA, Vienna, Austria, 567–584, 1967.